OPTICAL PROPERTIES OF CDSE THIN FILMS WITH DIFFERENT THICKNESSES OBTAINED BY THE METHOD OF HIGH-FREQUENCY MAGNETRON SPUTTERING

A. I. KASHUBA[1,a], H. A. ILCHUK[1], I. V. SEMKIV[1], B. ANDRIYEVSKY[2], Y. M. STOROZHUK[1], R. Y. PETRUS[1]

[1]Department of General Physics, Lviv Polytechnic National University,
S. Bandera 12, 79013, Lviv, Ukraine
Corresponding author[a]: andrii.i.kashuba@lpnu.ua
[2]Faculty of Electronics and Computer Sciences, Koszalin University of Technology,
Sniadeckich 2, 75-453, Koszalin, Poland

Received December 23, 2022

Abstract. The optical and structural properties of CdSe thin films with different thicknesses (0.02–0.73 μm) prepared by the high-frequency magnetron sputtering method are determined. The phase analysis and crystal structure refinement are performed using X-ray diffraction (XRD). All obtained CdSe thin films are crystallized in the cubic structure (ZnS – structure type) from XRD studies. The mean grain size of the films was determined using the Scherrer equation. The strain and the dislocation density are also calculated. The spectral dependence of the optical transmittance and reflectivity of the obtained sample in the visible and near-infrared regions is studied at room temperature. The normalized integral optical transmittance, reflectivity, optical band gap and the Urbach energy value of studied films are determined. The optical band gap values of CdSe thin films are changed between 1.57–2.32 eV (estimation from Tauc plot for CdSe with thicknesses 0.016–0.73 μm) and 1.62–1.66 eV (estimation from the dependence of dT/dλ *versus* wavelength λ for CdSe with thicknesses 0.242–0.73 μm). Optical properties (refractive index $n(\lambda)$, absorption coefficient $\alpha(\lambda)$, extinction coefficient $k(\lambda)$ and dielectric functions $\varepsilon(\lambda)$) of thin films and thickness d can be determined from the transmission spectrum. The dispersion of the refractive index was explained using a single oscillator model investigated. The material optical parameters such as static and high-frequency dielectric constant, the density of states effective mass ratio were also calculated. Dependence of the optical properties from the time of CdSe thin films deposition (thickness) is studied.

Key words: thin films, optical transmission, band gap, optical function.

1. INTRODUCTION

Taking into account the recent tendencies in modern electronics, one can witness that polycrystalline layers of semiconductors become more and more interesting for applications if compared with bulk semiconductors. Unlike single crystals or epitaxial structures, the synthesis of polycrystalline (both bulk and layered) semiconductors is characterized by a simpler and more efficient production process, which

requires neither highly precise growth equipment nor high-cost single-crystal substrates. These factors make semiconductor materials and devices based on the layers or thin films less expensive.

In particular, polycrystalline layers are of great interest for the developers of inexpensive solar cells for terrestrial applications. The authors of the works [1–3] rightfully affirm that the wide use of polycrystalline semiconductors in electronics has been limited for a long time by the availability of numerous extended defects such as grain boundaries or dislocations. At present, however, the current progress in the development of these materials has led to the situation when the polycrystallinity of the materials represents more hope for the future than a problem.

As an example, the grain boundaries in such semiconductors manifest specific electrical and recombination characteristics, which can be employed in a number of devices. Being a serious violation of the quality of the crystal lattice, these boundaries play a role of the effective internal getter that promotes removal of residual impurities and point defects from the bulk of the material. This property of intergrain boundaries can be used when improving operating characteristics of appropriate semiconductor-based electronic devices and, in particular, their thermal and radiation stability [4].

Thin films of cadmium chalcogenides (CdSe) represent a large $A^{II}B^{VI}$ group of crystalline materials that reveal a canonical semiconducting behavior. These materials embrace the large and important research field because of their wide application potential in various fields of optoelectronic devices.

To date, a great number of different techniques have been developed for preparing thin films of cadmium chalcogenides. These are physical vapor deposition, sputtering, spray pyrolysis, electro-deposition, close-space sublimation (CSS), etc. [5–11]. CdSe forms cubic and hexagonal phases, depending mainly on the choice of method for its synthesis and on the specific growth parameters [9–12].

Before, we are studies CdSe thin films with hexagonal structures deposited by close-space sublimation methods [9–11]. In this work, we change method of deposition for obtained CdSe thin films which are crystallized into cubic form. Some information about studies of the influence of thickness on optical properties of CdSe thin films was present in Ref. [13, 14]. In Ref. [13] CdSe thin films were deposited on ITO/glass substrates by electrodeposition method and obtained polycrystalline samples with cubic structure, but do not give spectral behavior of optical functions. A similar situation was realized in Ref. [14], but obtained CdSe thin films crystallized into the hexagonal structure. Nonetheless, the spectral behavior of optical parameters of CdSe thin films still needs further investigations. Note that all the above characteristics are important for optimizing the materials for solar power engineering.

The principal aim of the present work is to present the most important results concerned with the fundamental optical properties of CdSe thin films, crystallized

in cubic structures, with different thicknesses. Our main aim is to establish general features of the influence of the thicknesses of CdSe thin films on the structural and optical properties.

2. EXPERIMENTAL DETAILS

CdSe thin films were deposited on quartz substrates by the method of high-frequency (HF) magnetron sputtering ($\sim$ 13.6 MHz) using a VUP-5M vacuum station (Selmi, Ukraine). A single crystal disc of 99.99 $\%$ purity with a thickness of 2 mm and a diameter of 40 mm was used as a target. The target – substrate distance was 60 mm. The deposition time was 180, 360, 540, 720 and 1200 sec (label for samples from S1 to S5). The start and end of the process were controlled by means of a movable shutter. Before the sputtering process, the chamber was evacuated. The gas pressure inside the chamber was 4×10^{-4} Pa.

The sputtering was carried out at a pressure of argon (Ar) in the range of 1.0–1.3 Pa. The power of the HF magnetron was maintained at the level of 50 W and the temperature of the substrate at 489 K. For heating the substrates, a high-temperature tungsten heater with a power of 300 W was used. The temperature was controlled by means of a proportional–integral–derivative (PID) controller for controlling heating and cooling rates, as well as for ensuring the temperature conditions of deposition.

The phase analysis and crystal structure refinement was examined with X-ray diffraction data (XRD) obtained on DRON-2.0M diffractometer at room temperature with the Kα radiation (λ= 1.936087 angstrom) of Fe. The spectral dependence of the optical transmittance and reflectivity (Shimadzu UV-3600) of the obtained samples in the visible and near infrared regions (300–1500 nm) is studied at room temperature [9–11].

3. RESULTS AND DISCUSSION

3.1. STRUCTURE ANALYSIS

Crystal structure of CdSe thin films has been determined from XRD (see Fig. 1). The XRD (see Fig. 1) show that the all samples (except of the S4) have one intense reflection peak at approximately 32°. Sample S4 have less defined crystalline structure (weaker and broader peaks), but again the main peak is around 32°, and there are smaller peaks at about 54° and 64°. If compared these data with the references for cubic and hexagonal CdSe, we see that the main peak could belong to (1 1 1) plane of the cubic CdSe (the exact position is 31.313°). However, the peaks at 54° and 64° do not exist in cubic lattice (in the case of the S4 sample), but present

at the position 52.297° (corresponded to (2 2 0) plane) and 62.231° (corresponded to (3 1 1) plane), respectively. CdSe thin film crystallizes in cubic structure (structure type – ZnS, space group *F*-43*m*), with the unit-cell dimensions for different samples are listed in Table 1.

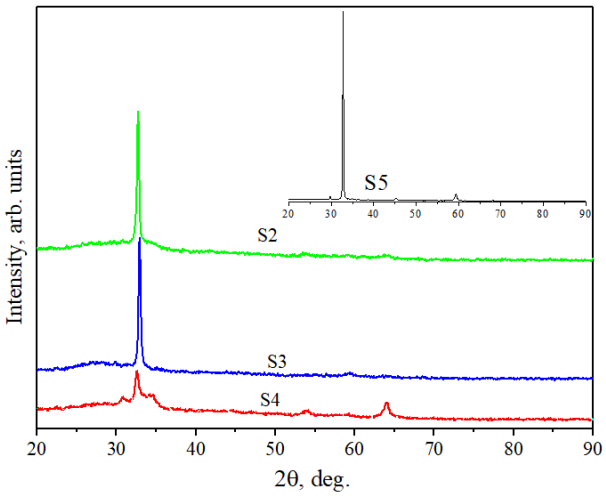

Fig. 1 – XRD pattern of CdSe (S2–S4, and in the inset for S5 sample) thin films.

The crystallite size (D) was estimated from the peaks broadening using Sherrer's equation [15]:

$$D = \frac{0.9\lambda}{B \cdot cos\theta}. \tag{1}$$

where λ is the wavelength of X-rays, B is the full-width half maximum (FWHM) and θ is the Bragg's angle. The strain (ε) and the dislocation density (δ) were calculated using the following relations [16]:

$$\varepsilon = \frac{B \cdot cos\theta}{4}, \delta = \frac{1}{D^2}. \tag{2}$$

We can be seeing (Table 1) that the average grain size for the studied films changed between 43 and 90 nm. The average grain size, dislocation density and strain shows a good correlation for CdSe thin films with a time of deposition below 9 minutes. The decrease in strain value (except S4) shows that there is a reduction in the concentration of imperfections created in the lattice with the increase in film thickness [13].

Table 1

Structure parameters of CdSe thin films (Structure type - ZnS; Space group - *F*-43*m*).

Sample	S2	S3	S4	S5
a, nm	0.59323(9)	0.59433(10)	0.59700(7)	0.59412(10)
V, nm^3	208.78(9)	209.94(11)	212.78(8)	209.71(11)
D, nm	67	69	43	90
δ, nm^{-2}	2.2 10^{-4}	2.1 10^{-4}	5.5 10^{-4}	1.2 10^{-4}
ε	6.5 10^{-2}	6.3 10^{-2}	0.11	4.9 10^{-2}

3.2. RESULTS OF THE OPTICAL MEASUREMENTS

The transmittance and reflection spectra of the CdSe thin films are presented in Fig. 2. The transmission and reflectivity spectra of the thin films exhibit periodic peaks and minimums associated with interference effects, indicating the high structural perfection of thin films. A very rough surface will destroy the interference due to multiple reflections.

For each film, full transmission and reflectivity spectra were calculated and the normalized integrated transmission and reflectivity to the CdSe absorber were evaluated as follows:

$$\overline{T} = \frac{1}{b\text{-}a}\int_a^b T d\lambda, \overline{R} = \frac{1}{b\text{-}a}\int_a^b R d\lambda \tag{3}$$

where, $\overline{T}$ and $\overline{R}$ are the average fractional transmission over the range *a*-*b* specified (see Fig. 2), respectively. The obtained values of integral transmission and reflectivity are listed in Table 2 (*a*= 300 nm, *b*= 1500 nm for transmission, *a*= 300 nm, *b*= 900 nm for reflectivity).

To determine the thickness of the films under investigation, we can use the following equation,

$$d = \frac{M\lambda_1\lambda_2}{2(n(\lambda_1)\lambda_2 - n(\lambda_2)\lambda_1)}, \tag{4}$$

where λ_1 and λ_2 are wavelengths corresponding to neighboring extreme points in the transmission spectrum and *M*= 1 for two neighboring extrema of one type (max–max, min–min) and *M*= 0.5 for two neighboring extrema of opposite types (max–min, min–max). The thickness of the CdSe thin films calculated by Eq. (4) is given in Table 2.

To estimate the absorption band edge energy of the films the first derivative of the optical transmittance can be used. The dependence of d*T*/dλ *versus* wavelength λ was plotted, as shown in Fig. 3. The position of the characteristic highest peak of d*T*/dλ corresponds to the optical band gap energy listed in Table 2. But, for ultrathin

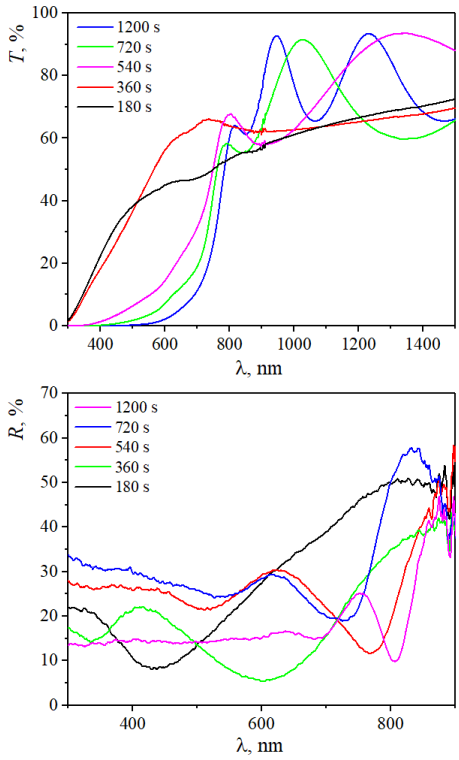

Fig. 2 – Transmittance (T) and reflection (R) spectrum of the CdSe thin films for different times of deposition (see legend).

films ($\leqslant$ 130 nm) we can not estimate the band gap by using this method. This is connected to the very high transmission of samples (see Table 2).

The optical band gap E_g has been determined also from the spectrum of the absorption coefficient $\alpha(h\nu)$. For this purpose the known Tauc relation for the direct optical transition between valence and conduction bands has been used [17],

$$(\alpha \cdot h\nu)^2 = A(h\nu - E_g), \tag{5}$$

where A is an energy-independent constant and $h\nu$ is the photon energy. Here, the absorption spectrum $\alpha(h\nu)$ has been calculated from transmittance data in the spectral range of stronger absorption [17]. The direct optical band gap E_g has been obtained by plotting the dependence $(\alpha \cdot h\nu)^2$ *versus* $h\nu$ and following a linear approximation of this dependence to the value $(\alpha \cdot h\nu)^2$= 0 (Fig. 4). Thus, we have evaluated the exact value of the direct optical band gap for the films studied being equal between 1.57 and 2.32 eV (see also Table 2). The estimated band gap values of the studied CdSe films obtained by the two above-mentioned methods show good correlation

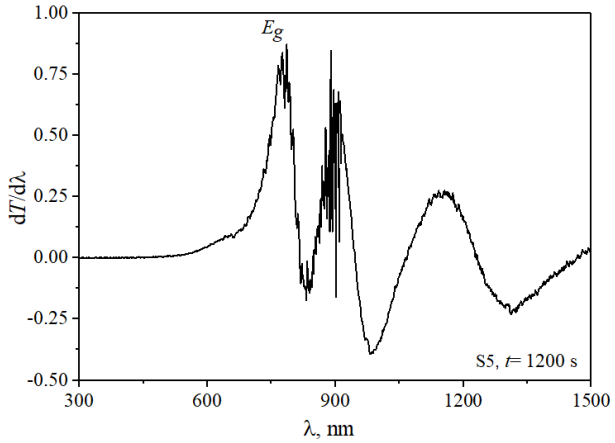

Fig. 3 – Wavelength spectrum of the transmittance derivative dT/dλ of CdSe thin films for different times of deposition (see legend).

(see Fig. 5). We found that samples with thickness smaller than 130 nm optical band gap shows increasing with decreasing thickness of CdSe thin films. This effect can be caused by the manifestation of the influence of size effect [18–23]. Increases in the optical band gap (from 1.8 to 2.21 eV) with a decrease in film thickness (from 600 to 350 nm) were also observed for CdSe thin films with a hexagonal structure [19].

These results indicate that a tendency to a certain narrowing in the gap against the thickness occurs and the absorption edge is red shift in thicker films. This behavior is mainly attributed to the carrier concentration (N) variations [19, 21–23]. The decrease in N with thickness can be ascribed to the increase in the grain size and the enhancement of the crystalline quality [20–23]. On the evidence of the XRD results (see Table 1), we are obtained increse of the grain size and the crystallinity when increasing of the film thickness increased.

When film thickness is small enough, two factors may play an important role: the small size of crystallites and their number per unit area of the substrate [20]. Also, one can expect that the E_g^{opt} decreases with increasing the film thickness because the crystal defects can be formed which produce localized states that change the effective Fermi level due to an increase in carrier concentrations [21]. The samples of lower thickness must contain much more defects which constitute can be important source of free carriers. As the grain size increases the amount of defects decreases to some extent leading, thus, to a decrease in the free carrier density [23].

The spectral dependence $\alpha(h\nu)$ near the band edge reveals an exponential dependence on the photon energy and follows Urbach's empirical Eq. (6),

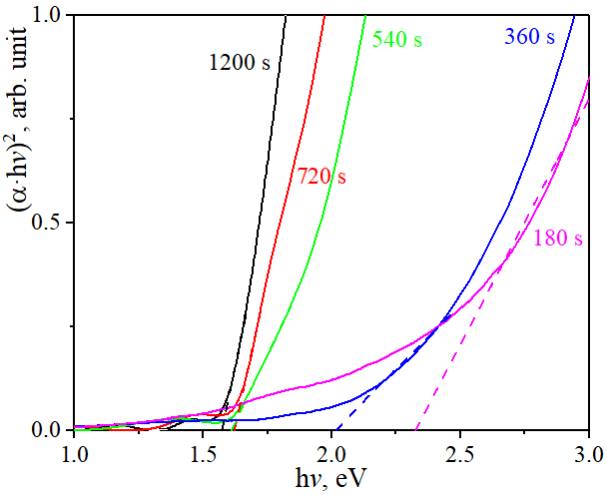

Fig. 4 – Absorption spectra α in presentation of $(\alpha \cdot h\nu)^2$ as function of photon energy $h\nu$.

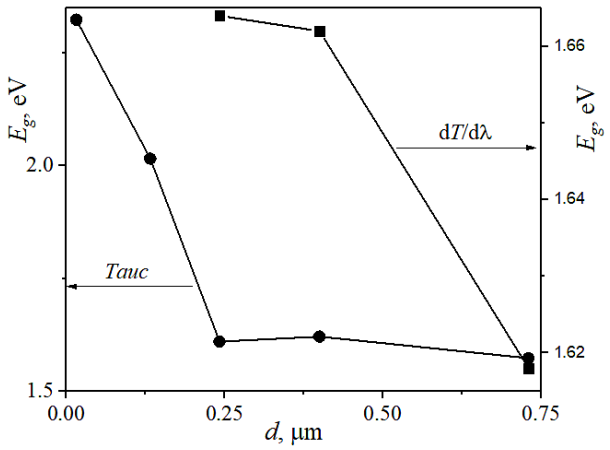

Fig. 5 – Thickness dependence of the optical band gap, estimation from Tauc coordinates (circle) and from dependence of dT/dλ *versus* wavelength λ (square).

$$\alpha(h\nu) = \alpha_0 exp(\frac{h\nu}{E_u}), \tag{6}$$

where α_0 and E_u (Urbach's energy) are the characteristic parameters of the material studied. One can determine the parameters α_0 and E_u from the experimental dependence $\alpha(h\nu)$. The value of Urbach's energy E_u depends on the structural disorder and temperature of the material. Temperature dependence of this energy is formed

by the interaction of electrons/excitons with optical phonons [24].

Table 2

Optical parameters of CdSe thin films.

Sample	S5	S4	S3	S2	S1
d, μm	0.73	0.40	0.24	0.13	0.02
$\triangle d$, μm	0.11	0.07	0.05	0.07	0.01
T_{ave}, %	47.40	45.31	52.72	55.36	52.72
R_{ave}, %	18.73	31.29	25.80	26.24	26.55
E_g, eV	1.57	1.62	1.61	2.016	2.32
E_g, eV [13]	1.74	1.80	1.89	1.93	-
d, nm	127	110	78	50	-
$E_g(\mathrm{d}T/\mathrm{d}\lambda)$, eV	1.62	1.66	1.66	-	-
E_u, eV	0.98	0.42	0.16	-	-

The optical properties of a thin film (refractive index $n(\lambda)$, absorption coefficient $\alpha(\lambda)$, extinction coefficient $k(\lambda)$, dielectric functions $\varepsilon(\lambda)$ and thickness d) can be easily evaluated from a transmission spectrum with interference effects using the envelope method [9, 25]. This method is applicable in the case of a weakly absorbing thin film on an entirely transparent substrate that is much thicker than the thin film. These conditions are met in this work.

The envelope curves $T_{max}(\lambda)$ and $T_{min}(\lambda)$ can be obtained by means of parabolic extrapolation of experimentally determined points that coincide with the location of interference maxima and minima (see Fig. 6). But, this method is using when obtained "interference" in transmission spectra. As result, in the next part of the article we are analyzing the optical properties of S3–S5 samples.

Refractive index $n(\lambda)$ of the CdSe thin films can be calculated using the following:

$$n = \sqrt{N + \sqrt{(N^2 - n_s^2)}}, N = 2n_s \frac{T_{max} - T_{min}}{T_{max} \cdot T_{min}} + \frac{2n_s^2 + 1}{2}, \tag{7}$$

where, n_s is the refractive index of the substrate:

$$n_s = \frac{1}{T_s} + \sqrt{(\frac{1}{T_s})^2 - 1}. \tag{8}$$

T_s is the transmittance of the substrate in the transparent zone. For the quart substrate T_s= 0.915, hence following the Eq. (8) n_s= 1.51 (transmission spectra of quartz substrate can be found in Ref. [26]).

The calculated refractive index n of the CdSe thin films studied decreases with increasing wavelength λ (Fig. 7). Here, the dispersion $n(\lambda)$ is normal and may be

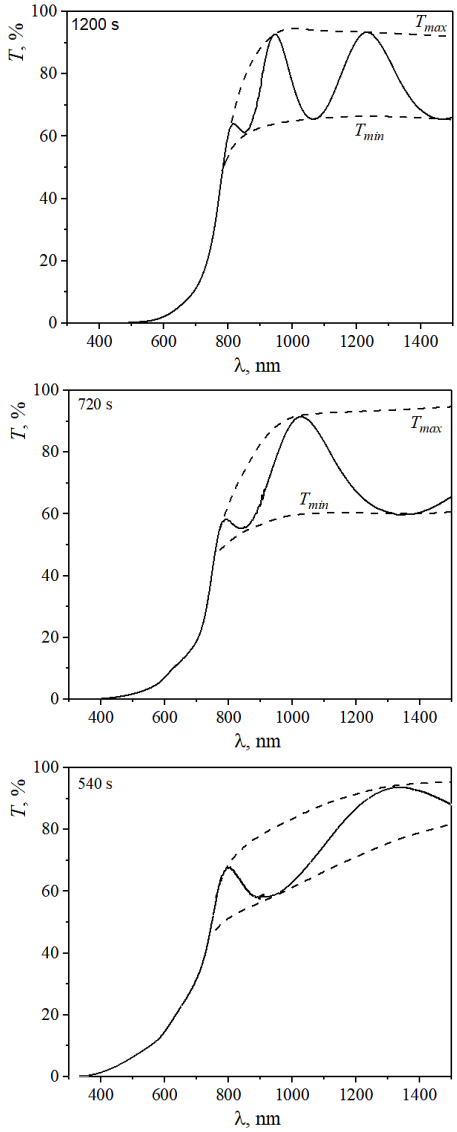

Fig. 6 – Transmission spectra of CdSe thin films with envelope curves.

well approximated by the single oscillator model. For analysis of spectral behavior of refraction index we are used a single oscillator model in the form proposed by Wemple and Di Domenico [27],

$$n^2(h\nu) - 1 \cong \frac{E_d E_0}{E_0^2 - (h\nu)^2} \tag{9}$$

where E_0 is the single oscillator energy (is an average energy gap), E_d is the dispersion energy (which is a measure of the strength of inter-band optical transitions) and $h\nu$ is the photon energy. Both parameters, E_0 and E_d, can be obtained from the parameters of the above-mentioned linear fit $(n^2(h\nu)\text{-}1)^{-1} \sim f(h\nu)^2$ of Eq. (9). The values of these parameters are summarized in Table 3.

The refractive index $n_0 = n(h\nu = 0)$ can be determined by using the expression $n_0 = \sqrt{1 + \frac{E_d}{E_0}}$. The value n_0 usually does not change with increased film thickness (see Table 3).

The M_{-1} and M_{-3} moments of the optical spectra can be obtained from the following relations [27]:

$$E_0^2 = \frac{M_{-1}}{M_{-3}}, E_d^2 = \frac{M_{-1}^3}{M_{-3}} \tag{10}$$

The obtained values are given in Table 3. In addition, the oscillator strength (f) is expressed according to Wemple and DiDomenico via the following formula [24]:

$$f = E_0 E_d \tag{11}$$

From analysis we can see that increases in film thickness lead to increasing fundamental optical parameters, such as single oscillator energy, dispersion energy and optical oscillator strength (Table 3).

The parameter E_d which is a measure of the strength of interband optical transitions obeys the simple empirical relationship:

$$E_d = \beta N_c Z_a N_e \tag{12}$$

N_c is the coordination number of the cation nearest neighbor to the anion, Z_a is the formal chemical valency of the anion, N_e is the effective number of valence electrons per anion. In our case, $N_c = 4$, $Z_a = 2$, $N_e = 8$. By using Eq. (12) we obtained "covalent" value between 0.44 and 0.47 eV. The occurrence of anomalously large values of E_d to contributions of the filled d band to interband transitions [28].

The refractive index dispersion $n(\lambda)$ in the range of transparency can be approximated also by using the Sellmeier dispersion equation Eq. (13) [29],

$$(n^2 - 1)^{-1} = \frac{1 - (\frac{\lambda_0}{\lambda})^2}{S_0 \lambda_0^2}, \tag{13}$$

where S_0 is the average oscillator strength and λ_0 is the average interband oscillator wavelength. When the dependence of $(n^2 - 1)^{-1}$ *vs.* λ^{-2} is plotted and the straight line fit is performed, then the values S_0 and λ_0 can be determined from Eq. (13) (see Table 3).

Table 3

Single oscillator parameters of CdSe thin films.

Sample	S5	S4	S3
E_0, eV	7.25	7.03	6.82
E_d, eV	30.11	29.21	28.21
n_0	2.27	2.27	2.27
M_{-1}	4.15	4.16	4.14
M_{-3}, eV^{-2}	0.08	0.08	0.09
f, eV^2	218.3	205.4	192.4
λ_0, nm	54.07	55.96	57.51
S_0, nm^{-2}	1.4 10^{-3}	1.3 10^{-3}	1.3 10^{-3}
β, eV	0.47	0.46	0.44

Absorption coefficient $\alpha(\lambda)$ for CdSe thin films can be calculated using the following equation:

$$\alpha(\lambda) = \frac{1}{d} ln\{\frac{(n-1)(n-n_s)((\frac{T_{max}}{T_{min}})^{1/2}+1)}{(n+1)(n+n_s)((\frac{T_{max}}{T_{min}})^{1/2}-1)}\} \tag{14}$$

Figure 7 shows the absorption coefficient α for the material of CdSe thin films as a function of the wavelength. A sharp increase in the absorption coefficients is observed in the short wavelength region near the band gap absorption edges of CdSe thin films.

The extinction coefficient $k(\lambda)$ can be easily calculated from the following equation $k(\lambda)= \lambda\alpha(\lambda)/4\pi$ (see Fig. 8). It can be seen from Fig. 8 that the extinction coefficients also increase sharply near band gap absorption edges.

The envelope method can be used only in the transparency region limits of a thin film. The following conditions are valid in a wavelength region near the self-absorption edge of CdSe thin films: strong absorption in the film material, a completely transparent substrate, and $n^2 >> k^2$.

It is known that the real and imaginary parts, ε_1 and ε_2 (see Fig. 9), of the complex dielectric permittivity ε:

$$\varepsilon = \varepsilon_1 + i \cdot \varepsilon_2 \tag{15}$$

are related to the refractive index n and extinction coefficient k by the Eqs. (16) and (17),

$$\varepsilon_1 = n^2 - k^2 \tag{16}$$

$$\varepsilon_2 = 2nk \tag{17}$$

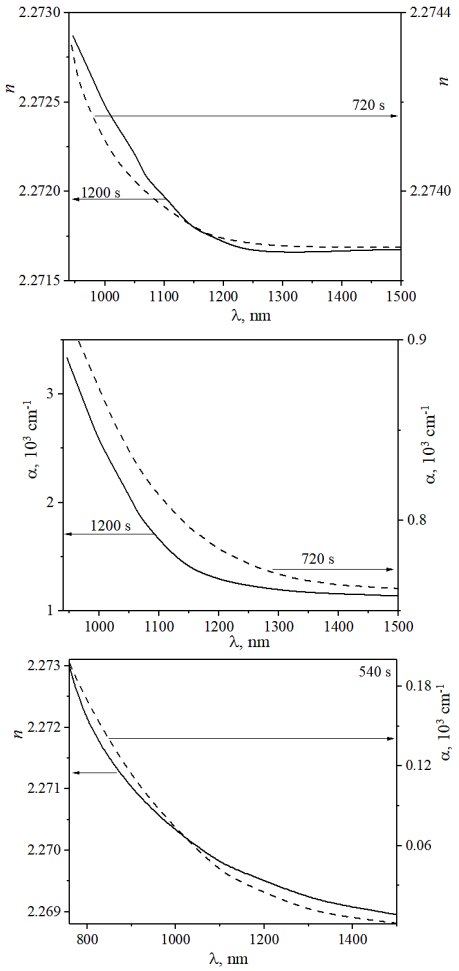

Fig. 7 – Refractive index and absorption coefficient depending on the wavelength of CdSe thin films (details marked on figures).

For the values of n much greater than k, the value ε_1 is approximately equal to n^2 and the dependence of $\varepsilon_1(\lambda)$ can be fitted using the relation [30] valid for the free electron's light absorption,

$$\varepsilon_1 = n^2 = \varepsilon_\infty - \left(\frac{e^2}{\pi c^2}\right) \cdot \left(\frac{N_c}{m^*}\right) \cdot \lambda^2, \tag{18}$$

where c is the speed of light, m^* is the effective mass of the carrier, N_c is the carrier density, e is the electronic charge and ε_∞ are the high-frequency dielectric constant. To obtain the high-frequency dielectric constant ε_∞ we plot a graph n^2 as a function

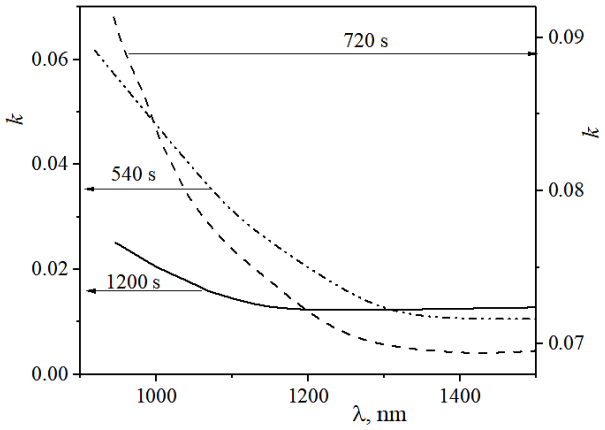

Fig. 8 – Extinction coefficient depending on the wavelength of CdSe thin films.

of λ^2 and extrapolated the linear part of the curve to $\lambda^2 = 0$ (see Table 4).

Table 4

Optoelectronic constants of CdSe thin films obtained from analysis of optical dielectric functions.

Sample	ε_∞	$\frac{N_c}{m^*}$, $\mathrm{kg}^{-1} \cdot \mathrm{m}^{-3}$
S5	5.16	$2.54\ 10^{45}$
S4	5.18	$2.23\ 10^{45}$
S3	5.16	$4.78\ 10^{46}$

4. CONCLUSION

CdSe thin films were deposited onto quartz substrates by the HF magnetron sputtering method. It is established that CdSe thin films are crystallized in the cubic structure from XRD studies. Crystallite size, strain, and dislocation density are calculated.

Optical characteristics of CdSe thin films with different thicknesses (0.016-0.73 μm) have been studied by the transmittance measurements in the wavelength spectral range of 300-1500 nm by the envelope method.

The data obtained have been used to calculate the optical band gap E_g, refractive index $n(\lambda)$, absorption coefficient $\alpha(\lambda)$, extinction coefficient $k(\lambda)$, complex dielectric function $\varepsilon=\varepsilon_1+i\varepsilon_2$ and several associated optical values of CdSe thin films. Found that for samples with the thickness smaller than 130 nm optical band gap

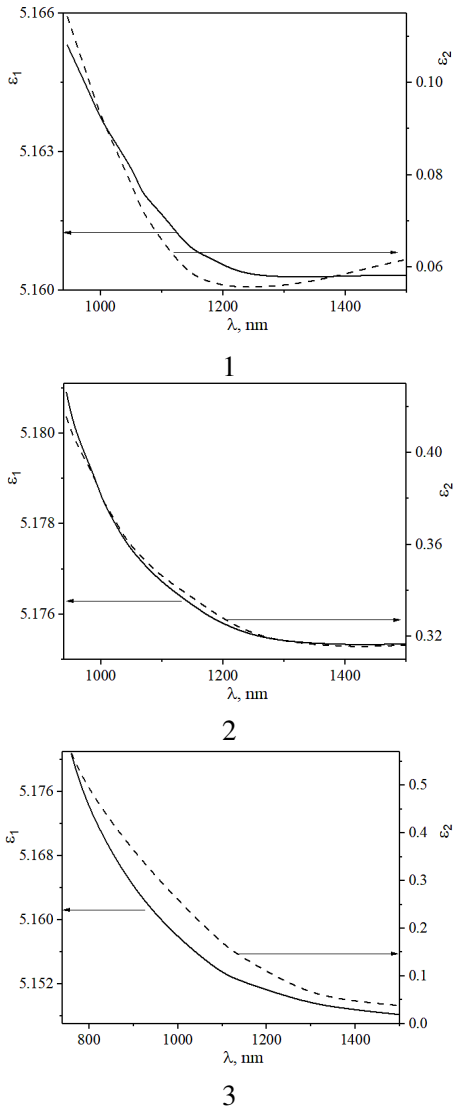

Fig. 9 – Real (ε_1) and imaginary (ε_2) parts of dielectric functions depending on the wavelength of CdSe thin films (1 - S5, 2 - S4, 3 - S3).

shows increasing with decreasing thickness of CdSe thin films. This effect can be caused by the manifestation the influence of the size effect.

One of the main findings is the increase in single oscillator energy, dispersion energy, optical oscillator strength value and Urbach energy for CdSe thin films with increasing thickness of samples.

Thickness dependence of ratio carrier density to the effective mass of the carrier for the CdSe thin films studied has been estimated for the first time. The increased thickness of CdSe thin films leads to a decrease in the ratio of carrier density to the effective mass of the carrier.

Acknowledgements. The work was supported by Project 0121U108649 of the Ministry of Education and Science of Ukraine.

REFERENCES

1. I. V. Kurilo, H. A. Ilchuk, S. V. Lukashuk, I. O. Rudyi, V. O. Ukrainets, N. V. Chekaylo, Semiconductors, **45**, 1531–1537 (2011).
2. S. A. Medvedev, Yu. V. Klevkov, C. A. Kolosov, V. S. Krivobok, A. F. Plotnikov, Fiz. Tekhn. Poluprov., **36**, 874–877 (2002).
3. N. L. Sermakasheva, G. F. Novikov, Yu. M. Shul'ga, V. N. Semenov, Semiconductors, **38**, 380–386 (2004).
4. M. G. Mil'vidskii, V. B. Ufimtsev, Inorg. Mater., **36** 287–292 (2000).
5. R. R. Guminilovych, P. I. Shapoval, I. I. Yatchyshyn, G. A. Il'chuk, V. V. Kusnezh, Russian Journal of Applied Chemistry, **86** 696–702 (2013).
6. P. K. Nair, M. T. S. Nair, V. M. Garcia, O. L. Arenas, Y. Pena, A. Castillo, I. T. Ayala, O. Gomezdaza, A. Sanchez, J. Campos, H. Hu, R. Suarez, M. E. Rincon, Solar Energy Mater. Solar Cells., **52**, 313–344 (1998).
7. I. A. Kariper, O. Baglayan, F. Godec, Acta Phys. Polon. A., **128** B-219–B-221 (2015).
8. C. Baban, G. I. Rusu, Appl. Surf. Sci., **211**, 6–12 (2003).
9. H. Ilchuk, R. Petrus, A. Kashuba, I. Semkiv, E. Zmiiovska, Molecular Crystals and Liquid Crystals, **699**, 1–8 (2020).
10. G. A. Il'chuk, R. Yu. Petrus, A. I. Kashuba, I. V. Semkiv, E. O. Zmiiovs'ka, Optics and Spectroscopy, **128**, 49–56 (2020).
11. H. A. Ilchuk, A. I. Kashuba, R. Y. Petrus, I. V. Semkiv, V. G. Haiduchok, Journal of Physical Studies, **24**, 3705(9) (2020).
12. S. V. Averin, P. I. Kuznetsov, V. A. Zhitov, N. V. Alkeev, V. M. Kotov, L. Y. Zakharov, N. B. Gladysheva, Techn. Phys., **57**, 1514–1518 (2012).
13. R. Choudhary, R. P. Chauhan, Journal of Materials Science: Materials in Electronics, **30**, 5753–5759 (2019).
14. Y. Akaltun, M. A. Yildirim, A. Ates, M. Yildirim, Optics Communications, **284**, 2307–2311 (2011).
15. P. Scherrer, Bestimmung der inneren Struktur und der Größe von Kolloidteilchen mittels Röntgenstrahlen. In: Kolloidchemie Ein Lehrbuch. Chemische Technologie in Einzeldarstellungen (Springer, Berlin, Heidelberg, 1912).
16. A. I. Kashuba, H. A. Ilchuk, R. Yu. Petrus, B. Andriyevsky, I. V. Semkiv, E. O. Zmiyovska, Applied Nanoscience (Switzerland), **12**, 335–342 (2022).
17. J. Tauc, R. Grigorovici, A. Vancu, Physica status solidi b, **15**, 627–637 (1966).
18. H. A. Ilchuk, A. I. Kashuba, R. Y. Petrus, I. V. Semkiv, V. M. Kordan, Nanosistemi, Nanomateriali, Nanotehnologii, **19**, 139–146 (2021).
19. M. Khammass Khalaf, B. A. M. Alhilli, A. I. Khudiar, A. Abd Alzahra, Photonics and Nanostructures - Fundamentals and Application, **18**, 59–66 (2016).

20. M. S. Shaalan, R. Muller, Solar Cells., **28**, 185–192 (1990).
21. D. Prakash, E. R. Shaaban, M. Shapaan, S. H. Mohamed, A. A. Othman, K. D. Verma, Materials Research Bulletin, **80**, 120–126 (2016).
22. A. Goktas, F. Aslan, E. Yasar, I. H. Mutlu, J Mater Sci: Mater Electron., **23**, 1361–1366 (2012).
23. M. Bouderbala, S. Hamzaoui, B. Amrani, A. H. Reshak, M. Adnane, T. Sahraoui, M. Zerdali, Physica B., **403**, 3326–3330 (2008).
24. A. Kocyigit, M. O. Erdal, M. Yildirim, Zeitschrift fur Naturforschung, **74**, 915–923 (2019).
25. R. Yavorskyi, L. Nykyruy, G. Wisz, P. Potera, S. Adamiak, Sz. Gorny, Applied Nanoscience (Switzerland), **9**, 715–724 (2018).
26. H. A. Ilchuk, A. I. Kashuba, R. Y. Petrus, I. V. Semkiv, N. A. Ukrainets, Physics and chemistry of solid state, **21**, 57–60 (2020).
27. S. H. Wemple, M. DiDomenico, Phys. Rev. B., **3**, 1338 (1971).
28. M. Born, E. Wolf, "Principles of Optics", Chap. II. (Pergamon Press: Oxford, 1975).
29. S. H. Wemple, Phys. Rev. B., **7**, 3767 (1973).
30. A. I. Kashuba, B. Andriyevsky, H. A. Ilchuk, R. Yu. Petrus, T. S. Malyi, I. V. Semkiv, Journal of nano- and electronic physics, **13**, 04006 (2021).